Available online at www.sciencedirect.com
ScienceDirect
Trans. Nonferrous Met. Soc. China 29(2019) 2340−2350
Transactions of Nonferrous Metals Society of China
www.tnmsc.cn

Influence of pile-up on nanoindentation measurements in Cu−2wt.%Be samples with precipitates

S. MONTECINOS[1,2], S. TOGNANA[1,3,4], W. SALGUEIRO[1,3,4]

1. IFIMAT, Facultad de Ciencias Exactas, Universidad Nacional del Centro de la Provincia de Buenos Aires, Pinto 399, 7000 Tandil, Argentina;
2. Consejo Nacional de Investigaciones Científicas y Técnicas CONICET, Av. Rivadavia 1917, C1033AAJ Buenos Aires, Argentina;
3. CIFICEN (UNCPBA-CICPBA-CONICET), Pinto 399, 7000 Tandil, Argentina;
4. Comisión de Investigaciones Científicas de la Provincia de Bs. As., Calle 526 entre 10 y 11, 1900 La Plata, Argentina

Received 22 February 2019; accepted 28 August 2019

Abstract: The influence of pile-up on the nanoindentation measurements in Cu−2wt.%Be samples with precipitates was carefully studied. The precipitates were formed by aging treatments for 1 h at different temperatures between 540 and 680 K. The load−depth curves were analyzed using the classical Oliver and Pharr method, and the obtained elastic modulus and hardness were compared with values estimated by other techniques. An important level of pile-up was found in samples with precipitates and differences in the load−depth curves were observed between the unaged and aged samples. A correction of the contact depth considering the pile-up proposed by Loubet was used for hardness estimation. For the determination of the elastic modulus, an approach based on the relation between the ratio of unloading work to indentation total work, with the ratio H/E_r (H is the hardness; E_r is the reduced modulus), was employed. A specific relation between both parameters was developed.

Key words: pile-up; nanoindentation measurement; copper alloy; precipitation; microstructure; mechanical properties

1 Introduction

The instrumented nanoindentation is a technique that allows the study and resolution of problems in the field of material science at nanometric scale. By this technique, the load−depth curve of each indentation can be obtained. The use of atomic force microscopy as a complement of the instrumented nanoindentation allows to obtain images of the surface after the indentation, which gives important information about the behavior of the material. Other authors have also performed finite element simulations of the indentations on a material to study the indentation response [1,2]. The analysis of the load−depth curves obtained from instrumented nano-indentation is usually done using the well-known method of Oliver and Pharr. The Oliver and Pharr method (O−P method) was developed to determine hardness and elastic modulus from instrumented indentation measurements. It was introduced in 1992 [3], and subsequently improved [4−6]. This method allows to determine the mechanical properties of a material directly from the load−depth (P–h) curve, without needing the imprint image of hardness. It is assumed that the deformation during loading is elastic and plastic in nature, while the unloading is only elastic. The unloading curves can be well approximated by the power law relationship:

$$P=A(h-h_f)^m \tag{1}$$

where A is a constant, m is the unloading exponent, which is constant for a sample under specific test conditions and h_f is the final depth (see Fig. 1). The elastic unloading stiffness, S, is defined as the slope of the unloading curve in the upper portion [3]. Then, the contact depth, h_c, can be determined as follows:

$$h_c = h_{max} - \epsilon \frac{P_{max}}{S} \tag{2}$$

where h_{max} is the maximum depth (see Fig. 1), and ϵ is a constant that depends on the geometry of the indenter and takes the value of 0.75 for a Berkovich indenter. In this way, the reduced modulus, E_r, can be obtained as

Corresponding author: S. MONTECINOS; Tel: +54-249-4385670; Fax: +54-249-4385679; E-mail: dmonteci@exa.unicen.edu.ar
DOI: 10.1016/S1003-6326(19)65140-X

follows:

$$E_r = S\frac{\sqrt{\pi}}{2\beta\sqrt{A_c}} \quad (3)$$

where β is a dimensionless correction factor, which considers the lateral displacement within the indentation and is slightly greater than unity, and A_c is the projected contact area, which depends on the contact depth and is determined from the calibration tip function. Thus, the elastic modulus estimated from the Oliver and Pharr method (E_{O-P}) can be obtained from the value of E_r, using the Poisson ratio of the indenter and the sample [3].

Knowing the projected contact area and the maximum load, P_{max}, the hardness, H is estimated from

$$H = \frac{P_{max}}{A_c} \quad (4)$$

The hardness obtained from this method is based on the contact area under load, unlike the traditional hardness determined from the area of the residual impression. The values determined by both methods can be different, especially for materials with significant elastic recovery during unloading.

At this point, it is important to mention that, although the O−P method is widely used, there are some issues in which this method cannot be used in its original form. One of them is that the method assumes an elastic unloading. Other problem that will be explained later is the presence of pile-up in the indentation. CHEN et al [5] found that the presence of pile-up is very sensitive to the loading rate in polycrystalline copper, with larger pile-up for tests at higher rates.

The Cu−2wt.%Be alloy is a material with special properties due to its high strength and hardness, good corrosion resistance, non-magnetic and non-sparking characteristics. These qualities are based on the improvement of their properties through the formation of precipitates by aging treatments from the Cu solid solution α phase [7−10]. The precipitation sequence has been extensively studied and includes the formation of at least three stages before the formation of the stable γ phase [11−14]:

Solid solution → Guinier−Preston zones → γ'' phase → γ' phase → γ phase

The Guinier−Preston zones are formed by coherent monolayers of beryllium [11,12]. Pile-up of these zones takes place for longer aging time and metastable γ'' phase with spherical shape is formed [12,15]. With increasing the aging time, the size of spherical γ'' precipitates increases, their shape changes to ellipsoids and they transform to metastable γ' phase [11,15]. The stable γ phase formation with $B2$ structure occurs for longer aging time [11,13].

Several studies have reported the modification of the physical properties of Cu−2wt.%Be alloys with aging treatments and the formation of different precipitates [7−10]. Generally, these modifications are characterized by the mechanical behavior of the material and the determination of some parameters like the hardness and the elastic modulus. In a recent work, the influence of the microstructure on the elastic modulus determined by the impulse excitation technique and Vickers hardness has been studied in an alloy submitted to thermal aging at different time up to 5 h, and temperatures in the range of 540 and 680 K [8]. To the best of our knowledge, no rigorous studies have been reported regarding microscale mechanical properties modifications in high-strength CuBe alloys through instrumented nanoindentation.

On the other hand, the interpretation of the nanoindentation curves and the determination of the elastic modulus and hardness using the commonly used Oliver and Pharr model are complex in age-hardenable materials due to the possible presence of pile-ups during nanoindentation.

In this study, the influence of pile-up on the nanoindentation measurements in Cu−2wt.%Be samples with precipitates was carefully studied. The precipitates were formed by aging treatments for 1 h at different temperatures between 540 and 680 K. A careful analysis was developed considering the properties of the material. Images of the topography of the indentations were collected and the presence of pile-up was observed. In order to analyze the results obtained from O−P method, a comparison with results obtained by other techniques was done. While the hardness was obtained using a Vickers microdurometer, and the elastic modulus was determined by the non-destructive dynamic method, the impulse excitation technique, IET. This technique allows to accurately obtain the elastic modulus of different materials. Some corrections were done to the application of the O−P method on the studied samples for the correct determination of the elastic modulus and hardness.

2 Experimental

A Cu−2wt.%Be commercial alloy with some impurity elements (Ni, Co and Si, with contents lower than 0.5%) was used in this work. The unified numbering system (UNS) number of the material was C17200. It was provided by Roberto Cordes S. A. as polycrystalline bars with 6 and 10 mm in diameter. Prior to the aging treatments, the samples were kept at 1113 K during 10 min and quenched into water at room temperature (around 293 K). The aging treatments consisted of heating at 540, 580, 623 and 676 K for 1 h followed by

quenching into water at room temperature.

For indentation measurements, samples around 2 mm in thickness were cut using an Isomet speed saw with a diamond disc from the bars with a diameter of 10 mm. The specimens were smoothened with 600 and 1000 grit emery paper and polished with alumina powder with 0.3 μm in size. Then, they were washed and subjected to an ultrasound treatment to eliminate superficial impurities.

Instrumented indentation was realized in accordance with ISO 14577−1 test method, with a Hysitron triboindenter using a Berkovich diamond indenter with an included angle of 142.3°. The measurements were done at room temperature under load control. For each sample, at least six tests separated by 10 μm from each other were performed on four different zones of each sample, obtaining at least 24 indentations for each sample. With this procedure, tests were carried out on different grains of the samples. No significant differences were found between measurements realized on different grains, therefore, average values will be reported. On each test, indentations with a maximum load of 9 mN, loading and unloading rates of 300 μN/s and without holding time were performed. The maximum load was determined considering that the roughness of the samples does not exceed 10% of the depth of indentation. The load−depth curves were obtained for each indentation. Micrographs of the samples after unloading were obtained by atomic force microscopy (AFM) using the Hysitron triboindenter. The projected contact area was determined using the calibration tip function performed on fused quartz for h_c between 150 and 600 nm as follows:

$$A_c(h_c)=24.5\,h_c^2+1635.8h_c \quad (5)$$

Conventional Vickers microhardness indentations were carried out using a Mitutoyo MVK−H11 under different loads.

The elastic modulus was determined from IET measurements, using a specifically developed device (more details in Ref. [16]) and longitudinal mode. A sample with a length of 132.5 mm and a diameter of 6 mm was used. It was previously heated at 1113 K for 3.5 h and then submitted to different aging treatments. After each treatment, the sample was homogenized at 1113 K for 10 min. This dynamic technique is based on the determination of the fundamental frequency (f) of the material applying Fourier analysis, and the calculation of the elastic modulus (E) from f. The vibration excitation was produced by the impact of a small ball at one end of the sample, and the signal was recorded using a commercial microphone, a system of amplification and a digital oscilloscope.

3 Results and discussion

Instrumented nanoindentation measurements were performed on samples unaged and aged at different temperatures for 1 h. According to a previous study of the same authors [8], the microstructure of the samples submitted to different aging temperatures carried out in the present work is known. The specimen with a previous heat treatment at 1113 K and without aging is in α phase, which corresponds to a FCC solid solution of Cu.

In samples aged for 1 h at 540, 580 and 623 K, the presence of the metastable γ'' phase is expectable. However, the precipitates would present some slight differences in the morphology and crystal structure for different temperatures. These differences were identified by MONTECINOS et al [8] using differential scanning calorimetry as a shift in the temperature of dissolution of γ'' phase. At higher aging temperatures, γ'' phase would grow and gradually change the shape from spheres to plates [8,15,17]. In the sample aged at 676 K for 1 h, the formation of metastable γ' precipitates is expected, which is reflected in the maximum Vickers microhardness value reached after aging for 45 min [8].

Some representative load−depth (P−h) curves of the samples unaged and aged at different temperatures for 1 h are presented in Fig. 1. At a maximum load of 9 mN, the small recovery depth reached for the samples with precipitates, of almost half of the specimen without aging, agrees with the hardening induced in the material by the presence of nanometric metastable precipitates γ'' and γ' [8]. At aging temperatures (T_{aging}) of 580 K and 623 K the curves are similar to those obtained at T_{aging} of 540 and 676 K, which are not included in Fig. 1.

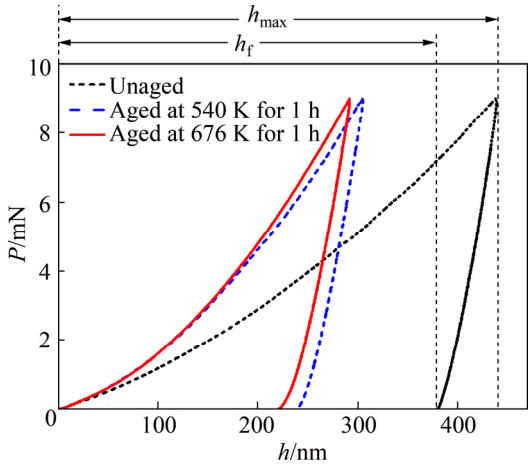

Fig. 1 Representative P−h curves obtained by instrumented nanoindentation of Cu−2wt.%Be specimens unaged and aged at 540 and 676 K for 1 h (h_{max} and h_f are indicated for unaged sample)

3.1 Pile-up

To analyze the accuracy and reliability of the elastic modulus and hardness values obtained by nano-indentation measurements and using the Oliver and Pharr method, a detailed analysis was performed, taking into account the considerations and limitations of this method.

The method proposed by OLIVER and PHARR [3,4] did not consider the pile-up of material that could occur at the contact periphery. In samples with pile-up in the indents, the real contact area would be larger than the projected contact area (A_c) estimated by the OLIVER and PHARR method [4]. That underestimation of the real contact area would lead to an overestimation of the elastic modulus and hardness [18].

Figures 2 and 3 show representative topographic images obtained by AFM of indentations performed on the samples unaged and aged at 580 K for 1 h, respectively. The sample without aging does not present pile-up (Fig. 2), while the presence of pile-up can be observed in all the specimens with precipitates. A representative indentation in an aged sample (at 580 K) is shown in Fig. 3. Following the procedure used by KIM et al [19], a quantification of the degree of pile-up in the samples can be estimated from the topographic images obtained by AFM, where h_{rp} is the indentation depth considering the deformed surface and h_m is the indentation depth with respect to the original surface, both after unloading (Fig. 3(b)). Both indentation depths were obtained as the average of the three sides for each indentation and in at least three representative zones of each sample. Therefore, the degree of pile-up of each sample was estimated as the average value of the ratio h_{rp}/h_m, and is presented in Fig. 4.

CHENG and CHENG [20,21] studied the validity of the Oliver and Pharr estimation for nanoindentation measurements. They found that this procedure can be used with confidence only for highly elastic materials, and should be used with caution for materials with a ratio $Y/E<10^{-2}$, where Y is the yield strength and E is the elastic modulus. For large Y/E values, sink-in would occur, while for small Y/E, both sink-in and pile-up may occur, depending on the work-hardening degree [20]. To estimate the Y/E ratio of each sample, reported values of the yield strength [7] and engineering stress−strain curves [22] for Cu−2wt.%Be samples were used. The elastic modulus was measured by IET (E_{IET}) for each sample. For the sample without aging, Y of 187 MPa was estimated as an average of the data from the literature. By a comparison of the Vickers microhardness determined for each sample and the yield strength values reported in the literature for the samples with precipitates and comparable aging treatments [7,22], an empirical relationship between hardness H_V and Y was estimated: $H_V/Y\approx3.2$. Other authors have reported values between 2 and 8 for this ratio in different materials, but values close to 3 are generally used [23−25]. It is important to note that in the sample without precipitates a higher ratio is obtained, and for the samples submitted to different aging treatments similar ratios are estimated. The values of Y/E_{IET} determined using the reported yield strengths are similar to those using the estimation of Y from H_V,

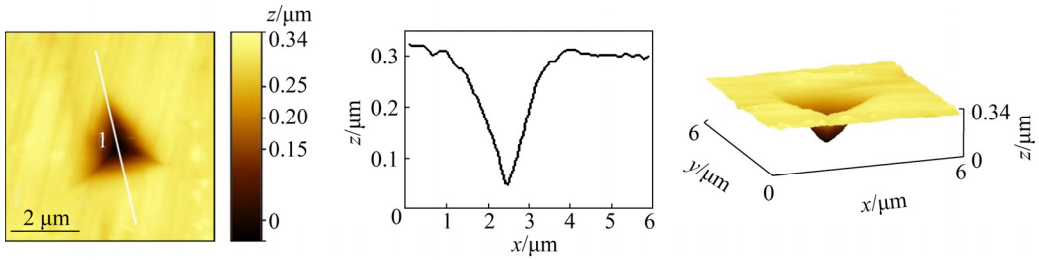

(a) (b) (c)

Fig. 2 Representative topographic image obtained by AFM on sample without aging after indentation (a), surface depth profile along selected line (b) and 3D image (c) of (a)

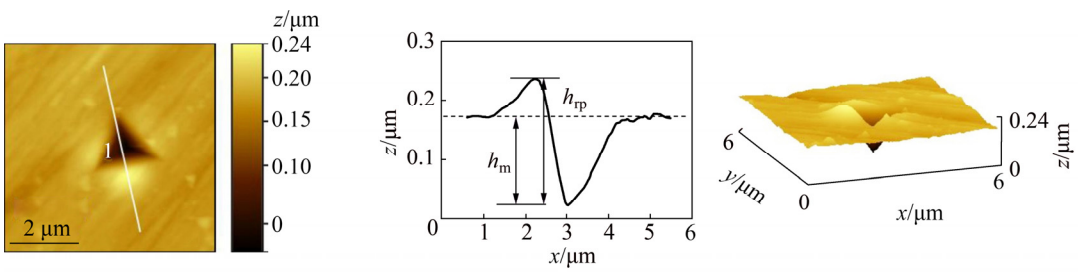

(a) (b) (c)

Fig. 3 Representative topographic image obtained by AFM on sample aged at 580 K for 1 h after indentation (a), surface depth profile along selected line (b) and 3D image (c) of (a)

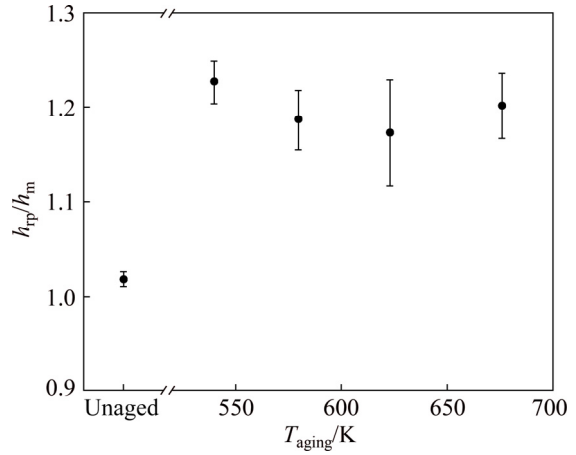

Fig. 4 h_{rp}/h_m ratios obtained from topographic images of Cu−2wt.%Be specimens unaged and aged at different T_{aging} for 1 h

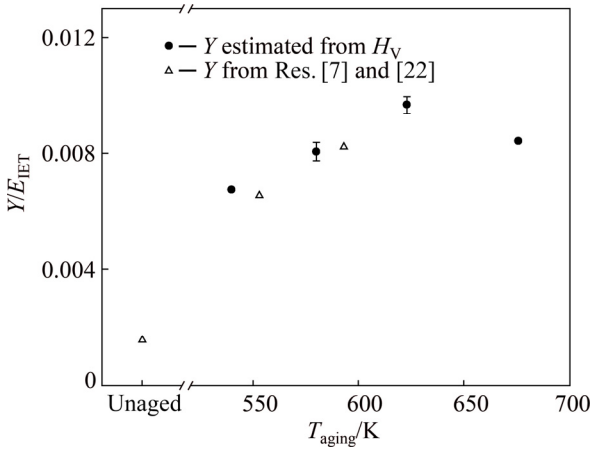

Fig. 5 Variation of Y/E_{IET} ratio with aging temperature for Cu−2wt.%Be specimens unaged and aged at different temperatures for 1 h (Y was estimated from the empirical relationship with H_V. The values of Y/E_{IET} with the yield strength obtained from Refs. [7,22] are also included)

and all of them are included in Fig. 5. For all the specimens Y/E_{IET} is approximately in the range of 10^{-3}−10^{-2}. The small values of Y/E for the studied alloy would cause errors in the application of the Oliver and Pharr procedure, which would be more significant due to the occurrence of pile-up in the specimens with precipitates [20].

Otherwise, the σ–ε (stress−strain) behavior of an elastoplastic metal under uniaxial tension is commonly assumed as

$$\begin{cases}\sigma = E\varepsilon,\ \sigma \le Y \\ \sigma = K\varepsilon^n,\ \sigma > Y\end{cases} \tag{6}$$

where K is the strength coefficient, and n is the work-hardening exponent. By using the engineering stress−strain curves of Cu−2wt.%Be samples reported by PANG et al [22], and using Eq. (6), values of n=0.25 and n=0.16 were obtained for the solution-treated specimen and that aged at 553 K for 20 min, respectively. These values indicate that the sample with hard precipitates exhibits a lower level of work-hardening with respect to the solution-treated sample. CHENG and CHENG [20,21] reported the relationship between Y/E, n and the pile-up level, which were obtained from the finite element method. They found that in samples with lower n, a higher pile-up is obtained, and for a given n a higher pile-up is observed for materials with lower Y/E ratio. However, the exact relationship between those parameters is still under discussion and most of the conclusions in the literature are based on element finite simulations. Nevertheless, the authors agree that at n values around 0.3 there is no pile-up or sink-in at Y/E≈0.01. This would be the case of the Cu−2wt.%Be sample without aging. For aged samples, the Y/E ratio increases, as is observed in Fig. 5. If a proportionality between H_V and Y is assumed, the Y/E ratio is expected to be more than twice that of the sample without aging. Following the results given by some authors [6,20,21], the value of n should decrease strongly to achieve a pile-up as that shown in Fig. 4.

According to these results, Cu−2wt.%Be specimens without precipitates do not exhibit pile-up or sink-in after the indentations. This behavior agrees with that reported for annealed polycrystalline Cu under slow loading rate [5,24]. On the other hand, the samples with precipitates exhibit the presence of pile-up after the indentations. The precipitates would act as a barrier against the dislocation motion, which results in an increase of hardness. During indentation, plastic deformation could not be accommodated into the bulk volume of the material due to this barrier effect, and the plastic zone is confined to the area near the indentation, which results in the presence of pile-up.

3.2 Hardness

From the nanoindentation curves, hardness ($H_{O–P}$) was determined using the Oliver and Pharr method [3,4]. OLIVER and PHARR [3,4] estimated h_c from Eq. (2). In Fig. 6, the Vickers microhardness values for a load of 300 g ($H_{V0.3}$) and $H_{O–P}$ for a sample unaged and samples aged at different temperatures for 1 h are presented. Both measurements exhibit similar behavior as a function of the aging temperature. It is worth noting that it is not expected that both measurements give the same values, because the hardness is determined from different methods and the levels of maximum applied load are also very different. For samples aged up to 623 K, the Vickers microhardness increases with the increase of the aging time due to the increase of the γ'' precipitates volume fraction up to 1 h [16]. For aging time more than 1 h, the

hardness is approximately constant. On the other hand, the sample aged at 676 K reaches a maximum of Vickers microhardness after 45 min, and for longer time, the hardness decreases with the increase of aging time, as was reported by MONTECINOS et al [8]. As a result, the sample aged at 676 K for 1 h exhibits a lower hardness value than that aged at 623 K.

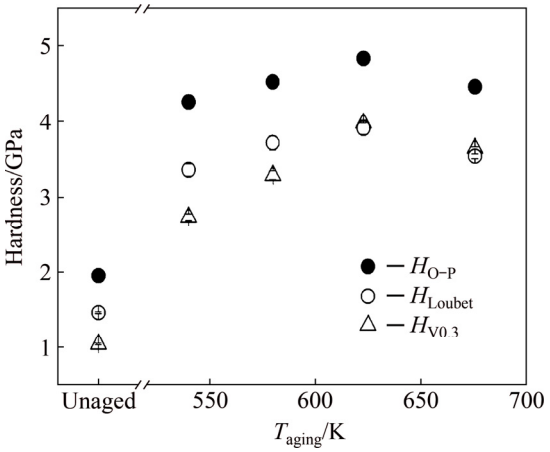

Fig. 6 Hardness values estimated using h_c (H_{O-P}), h_c^* (H_{Loubet}), and those obtained from Vickers measurements ($H_{V0.3}$) for Cu−2wt.%Be specimens unaged and aged at different temperatures for 1 h

For all the samples, higher values are obtained using the nanoindentation measurements with respect to Vickers microhardness. This fact has been previously reported by other authors [4,23]. It is important to note that H_{O-P} is defined as the mean pressure, of which the material will support under load [3], while the Vickers microhardness is based on the residual hardness impression.

The Oliver and Pharr method [3,4] can be used to calculate h_c of samples with sink-in between the specimen and the tip. As discussed above, the use of h_c calculated from the Oliver and Pharr method in the studied Cu−2wt.%Be alloy would cause errors in the estimation of the parameters of the material. Alternatively, LOUBET et al [26] proposed a model to calculate the contact depth in samples with pile-up deformation mode:

$$h_c^* = \alpha(h_{max} - \frac{P_{max}}{S}) \quad (7)$$

where α is a constant that depends on the indenter geometry and takes the value of 1.2 for a Berkovich tip [27−29]. The contact depth values obtained using the Oliver and Pharr method and those estimated from the Loubet model for the samples unaged and aged at different temperatures for 1 h are presented in Fig. 7. h_{max} is also included in this figure. As is expected, for all the samples, h_c^* presents values higher than h_c. In the samples with precipitates, h_c^* even takes values almost as high as h_{max}, which agrees with the presence of pile-up. For the sample unaged, h_c^* is higher than h_{max}, which indicates that the estimation by Loubet model would overestimate the value of the contact depth. This agrees with the observations with AFM, where pile-up almost does not occur in this sample.

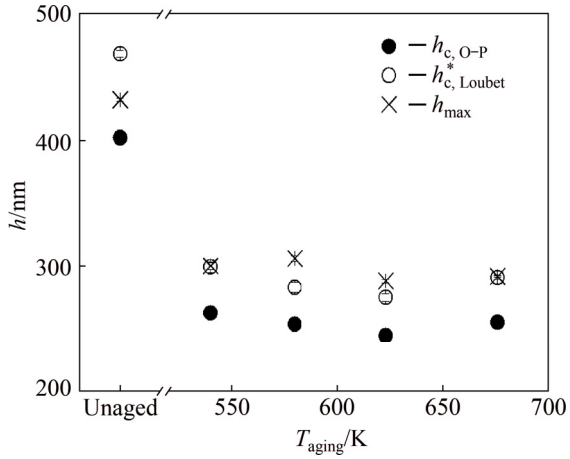

Fig. 7 Contact depth values obtained from Oliver and Pharr method ($h_{c,O-P}$), Loubet model ($h^*_{c,Loubet}$), and h_{max} for Cu−2wt.%Be specimens unaged and aged at different temperatures for 1 h

The hardness values obtained using Eq. (4), but determining the projected area as $A_c(h_c^*)$ from Eq. (5), are presented in Fig. 6 as H_{Loubet} along with the values of H_{O-P}. The hardness obtained considering the pile-up of the material, H_{Loubet}, presents values closer to those determined from the traditional method ($H_{V0.3}$). It is needed to mention that the definition of hardness obtained from Eq. (4) is different from the traditional hardness estimated from the imprint image, and some differences between both values would be expected, especially in materials with small Y/E ratio values [4]. Another effect that could influence the differences between both estimations of hardness is the dependence of H on the applied load. A load of 9 mN was employed for the nanoindentation curves, while a load of 3000 mN was used for Vickers measurements. According to Refs. [3,23,28], especially in copper-based alloys, it is expectable that the hardness decreases for higher loads due to the indentation size effect. This has been attributed to the increase of the geometrically necessary dislocations in small indentations which present large strain gradients. For example, the Vickers microhardness of the sample without aging treatment is decreased by 10% when the applied load changes from 500 to 3000 mN.

For the determination of the hardness in the Cu−2wt.%Be alloy, the Oliver and Pharr method would be the most appropriate for the sample without aging,

while H_{Loubet} would be a better estimation of the hardness for the samples with precipitates exhibiting pile-up.

3.3 Elastic modulus

The reduced elastic modulus of each sample (E_r) was estimated from the unloading curves using the Oliver and Pharr method and the software Hysitron Triboscan. From the values of E_r and using the relationship reported in Ref. [3], the elastic modulus ($E_{O–P}$) of each specimen was calculated. The following parameters associated to the indenter, which correspond to those of the diamond, were used: E_i =1141 GPa and ν_i=0.07 [3]. The Poisson ratio for Cu−2wt.%Be is assumed as ν=0.35 [8]. The values of $E_{O–P}$ obtained for the specimen without aging and samples aged at different temperatures for 1 h are presented in Fig. 8(a). $E_{O–P}$ exhibits a non-monotonic behavior with aging temperature.

The elastic modulus measured by IET (E_{IET}) for each sample is also included in Fig. 8(a). Each value corresponds to the average of at least 10 measurements. It can be observed that the modulus increases linearly with the increase of the aging temperature. This behavior

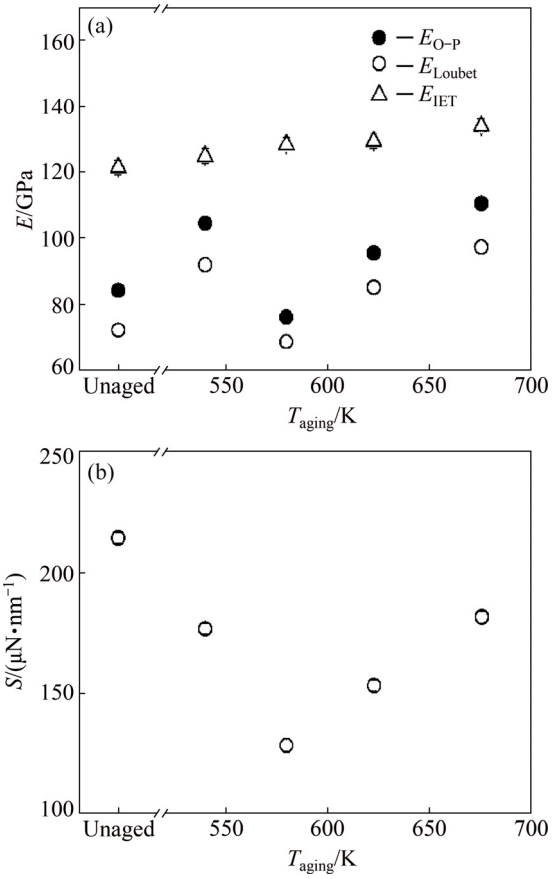

Fig. 8 Elastic modulus obtained by nanoindentation using Oliver and Pharr method ($E_{O–P}$), Loubet correction (E_{Loubet}) and by IET (E_{IET}) in Cu−2wt.%Be specimens unaged and aged at different temperatures for 1 h (a) and elastic unloading stiffness (S) determined for same specimens (b)

is associated with the increase of the fraction of precipitates for aging treatments at a fixed time and higher aging temperatures, as reported in Ref. [8].

To analyze the differences of the elastic modulus estimated from the Oliver and Pharr method and that obtained by IET, it is worth noting that the reduced modulus is calculated from S and A_c using Eq. (3) for the first method. As noted above, the Cu−2wt.%Be samples, especially those with precipitates, exhibit pile-up and the Loubet model is the most appropriate to determine the contact depth and with this value to obtain A_c. The modulus determined using this correction, E_{Loubet}, is presented in Fig. 8(a) to compare with $E_{O–P}$ and E_{IET}. Even with the Loubet contact depth correction, the elastic modulus presents a behavior with the aging temperature different from that shown by the IET measurements. The elastic unloading stiffness (S) determined from the load−depth curves as a function of aging temperature is presented in Fig. 8(b), with a behavior similar to that of $E_{O–P}$ for the samples with precipitates. The values of S shown in Fig. 8(b) were determined from an adjustment of the unloading curve using Eq. (1) and the subsequent calculation of the derivative. On the other hand, to discard possible numerical errors, S was also obtained from a linear fitting of the upper portion of the unloading curves, observing that both methods give similar values. These results suggest that the assumption that the unloading is completely elastic cannot be used in the studied material, especially in the samples with precipitates. On the other hand, the presence of a negative slope at start of unloading, in a small scale in our case, has been observed as a problem for the calculation of S [27].

On the other hand, CHENG and CHENG [21] studied the relationship between hardness, elastic modulus, and the work of indentation. The work of indentation can be obtained from the areas under loading−unloading curves of instrumented indentation measurements, where W_{tot} is the total work done by the indenter, and W_u is the work done by the solid to the indenter during unloading. Based on numerical simulations, some studies have proposed a correlation between the ratio of elastic recovery work to total work, W_u/W_{tot}, and the ratio of hardness to the reduced elastic modulus, H/E_r [21,29,30]:

$$\frac{W_u}{W_{tot}} = C_\theta \left(\frac{H}{E_r} \right) \tag{8}$$

where C_θ is a dimensionless function, which depends on the indenter angle. This correlation for the Cu−2wt.%Be alloy and considering the values of H_{Loubet} for the samples with precipitates and $H_{O–P}$ for the sample in α phase, and the reduced modulus obtained by IET, $E_{r\text{-}IET}$, is presented in Fig. 9. A linear dependence is observed

between the data of the sample in α phase and those with precipitates, being in agreement with the relationship presented in Eq. (8). A value of $C_\theta \approx 10$ is obtained. Using finite element simulations of a wide variety of elastic−plastic materials and conical indenter, CHENG and CHENG [21] reported a single value of $C_\theta \approx 5$, while N′JOCK et al [29] found C_θ values of 5.17 and 7.30, depending on the ratio W_u/W_{tot}, using a Vickers indenter on several materials. The importance of this method is that it is proposed to be used for samples where pile-up is large, instead of the traditional method developed by Oliver and Pharr, and the value of C_θ is independent of the work-hardening behavior [21].

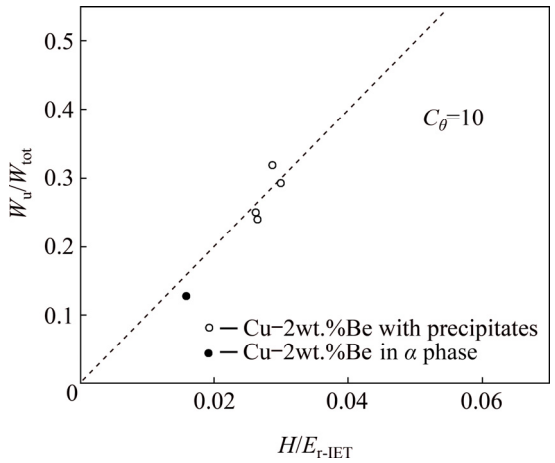

Fig. 9 Relationship between W_u/W_{tot} and $H/E_{r\text{-IET}}$ for Cu−2wt.%Be specimens in α phase and with precipitates (Dotted line corresponds to Eq. (8) for C_θ=10)

To know the conditions under which Eq. (8) is valid and understand the differences observed in the values of C_θ, a detailed analysis of the relationship between W_u/W_{tot} and H/E_r is done. CHEN and BULL [30] reported the following expression obtained for conical indenters:

$$\frac{W_u}{W_{tot}}=\frac{3m}{2(m+1)}\frac{\pi\tan\theta}{\beta}\frac{h_c}{h_{max}}\frac{H}{E_r} \tag{9}$$

where θ is the half-included angle of the conical indenter. Assuming that m is a constant with the value of 2 and the ratio $h_c/h_{max}=2/\pi$ [30] (according to the estimation given by Sneddon for an elastic contact), Eq. (9) can be simplified to the following:

$$\frac{W_u}{W_{tot}}=\frac{2\tan\theta}{\beta}\frac{H}{E_r} \tag{10}$$

For a conical indenter with θ=70.3° and using the value of β=1.065, CHEN and BULL [30] obtained a parameter $C_\theta \approx 5.25$ from Eq. (10), similar to the value reported by other authors.

To obtain the relationship between W_u/W_{tot} and H/E_r for the Cu−2wt.%Be alloy under study and using a Berkovich indenter, a methodology similar to that used to derive Eq. (10) will be used. It is commonly accepted that after plastic deformation occurs during loading with sharp indenters, the load−depth curve follows Kick's law [21,30,31]:

$$P_{load}=Ch^2 \tag{11}$$

while the unloading curves can be accurately described by the power law defined in Eq. (1). W_{tot} and W_u can be derived by integrating Eq. (11) and (1), respectively:

$$W_{tot}=1/3P_{max}h_{max} \tag{12}$$

$$W_u=\frac{P_{max}(h_{max}-h_f)}{m+1} \tag{13}$$

Thus,

$$\frac{W_u}{W_{tot}}=\frac{3}{m+1}\left(\frac{h_{max}-h_f}{h_{max}}\right) \tag{14}$$

On the other hand, the loading stiffness, S_l, and the unloading stiffness, S_u, at peak load can be obtained by differentiating Eqs. (11) and (1), respectively, with respect to h and evaluating at the maximum depth. In this way, the ratio between S_l and S_u is given by

$$\frac{S_l}{S_u}=\frac{2}{m}\left(\frac{h_{max}-h_f}{h_{max}}\right) \tag{15}$$

According to Ref. [4] and based on Sneddon's analysis, S_u can be also obtained through the following relationship:

$$S_u=\beta\frac{2}{\sqrt{\pi}}E_r\sqrt{A_c} \tag{16}$$

Thus, the ratio between S_l and S_u can be also given by

$$\frac{S_l}{S_u}=\frac{2P_{max}}{h_{max}}=\frac{\sqrt{\pi}}{2\beta E_r\sqrt{A_c}} \tag{17}$$

Combining Eqs. (14), (15) and (17), and the definition of hardness given in Eq. (4), we obtain

$$\frac{W_u}{W_{tot}}=\frac{3m}{2(m+1)}\frac{\sqrt{\pi A_c}}{h_{max}\beta}\frac{H}{E_r}=C_\theta\frac{H}{E_r} \tag{18}$$

It is important to note that the expression in Eq. (18) can be applied to any indenter, taking care to make necessary corrections in the calculation of the contact area.

Because the estimation of m from the experimental curves is too sensitive to the estimation procedure, we considered the sample without precipitates and chose the value of m=1.7, from which the value of the elastic modulus is the same using Eq. (18) and from IET measurements. If we assume that β=1.05 (as was determined by OLIVER and PHARR [4]), h_{max} is

determined from the P−h curves, and A_c is determined using the calibration tip function, Eq. (5), evaluated in the contact depth obtained by Loubet method, Eq. (7), for the samples with precipitates, and by the Oliver and Pharr method, Eq. (2), for the sample in α phase, C_θ is determined for each sample. The obtained C_θ values are presented in Fig. 10(a). These values are close to those obtained from experimental data in Fig. 9 of $C_\theta \approx 10$. It can be observed that specimens with higher differences and variability exhibit pile-up, which indicates that even with the corrections, this effect has some influence on the function C_θ estimated. The pile-up would affect the shape of the load−depth curves, deviating them from the behavior of the ideal elastic−plastic curves, especially in the unloading curves. The values of the elastic modulus calculated using C_θ for each sample according to Eq. (18) for the reduced modulus and then using the Oliver and Pharr relationship reported in Ref. [3] to determine elastic modulus $E_{C\theta}$, are presented in Fig. 10(b). The values of $E_{C\theta}$ are near to E_{IET}, obtaining an improvement with respect to the values determined from Oliver and Pharr method. However, some variability can be observed in the samples with pile-up, with the highest deviation respect to E_{IET} for the sample aged at 580 and 623 K. This deviation could be attributed to the differences in the microstructure of the samples. The specimens aged at 540, 580 and 623 K for 1 h have γ'' precipitates, while the sample aged at 676 K has main γ' precipitates [8]. The measurements indicate that when indentation is developed in samples containing γ' phase, the $E_{C\theta}$ determination is closer to E_{IET} than those containing γ'' precipitates. However, a good estimation is obtained in the sample aged at 540 K, probably because the volume fraction of γ'' phase (around 5%) is lower than that of the samples aged at 580 and 623 K (around 12%) [8]. One of the factors that have influence on the better determination of the elastic modulus in the samples with γ' phase is that they have an ellipsoid or plate shape with respect to the γ'' precipitates, which have sphere-shape [15]. This has influence on the better estimation of the modulus in the sample aged at 623 K with respect to that aged at 580 K because the shape of the precipitates formed at the highest aging temperature would be more similar to the ellipsoidal shape, according to Ref. [8]. However, more work is needed in order to understand the effect of different types of precipitates (shape and orientation) on the variability of the determined elastic modulus.

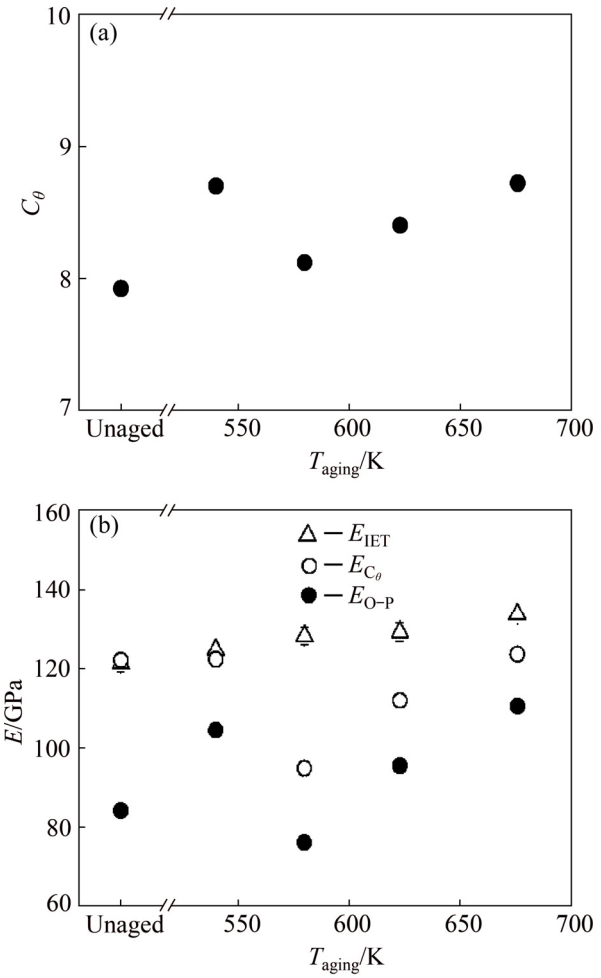

Fig. 10 C_θ obtained for each sample from Eq. (18) using m=1.7, β=1.05 and $A_c(h_c^*)$ for samples with precipitates and $A_c(h_c)$ for sample in α phase, and h_{max} of each P−h curve (a) and elastic modulus obtained from Eq. (18) and Oliver and Pharr relationship reported in Ref. [3] ($E_{C\theta}$) and compared with E_{IET} and E_{O-P} (b)

4 Conclusions

(1) Important differences in the load−depth curves were observed between the Cu−2wt.%Be samples unaged and aged. The surface after the indentation was analyzed. It is found that there is an important level of pile-up in samples with precipitates. This behavior is associated with a decrease of the work-hardening exponent in the samples with precipitates with respect to the others without aging.

(2) The hardness was estimated from the load−depth curves using the correction in the determination of the contact depth proposed by Loubet considering the pile-up. With this correction the hardness behavior was similar to that of Vickers microhardness for the samples with precipitates.

(3) A different approach was employed for elastic modulus (E) determination, based on the relationship between the ratio of unloading work to indentation total work, with the ratio H/E_r. A specific relationship between both parameters was developed and E was determined taking the area as input under the curve and the contact

area determined using the Loubet correction for the samples that exhibit pile-up. The values determined are close to those obtained using IET, mainly in the samples without aging and those with γ' precipitates.

Acknowledgments

This work was supported by Consejo Nacional de Investigaciones Científicas y Técnicas (CONICET), Comisión de Investigaciones Científicas de la Provincia de Buenos Aires (CICPBA), and SECAT (UNCPBA) Argentina. The authors would also like to thank to Bernardo Daga for his collaboration with the nanoindentation measurements and Techn. Dora Granate for her collaboration with the sample preparation for hardness measurements.

References

[1] HUI Y U, WU Jian-jun, WANG Ming-zhi, ZHAN Xue-peng, FAN He. Equivalent strain hardening exponent of anisotropic materials based on spherical indentation response [J]. Transactions of Nonferrous Metals Society of China, 2019, 29(1): 77−87.

[2] MA Yong, ZHANG Ying, YU Hai-feng, ZHANG Xiang-yu, SHU Xue-feng, TANG Bin. Plastic characterization of metals by combining nanoindentation test and finite element simulation [J]. Transactions of Nonferrous Metals Society of China, 2013, 23(8): 2368−2373.

[3] OLIVER W C, PHARR G M. An improved technique for determining hardness and elastic modulus using load and displacement sensing indentation experiments [J]. Journal of Materials Research, 1992, 7(6): 1564−1583.

[4] OLIVER W C, PHARR G M. Measurement of hardness and elastic modulus by instrumented indentation: Advances in understanding and refinements to methodology [J]. Journal of Materials Research, 2004, 19(1): 3−20.

[5] CHEN J, SHEN Y, LIU W, BEAKE B D, SHI X, WANG Z, ZHANG Y, GUO X. Effects of loading rate on development of pile-up during indentation creep of polycrystalline copper [J]. Materials Science and Engineering A, 2016, 656: 216−221.

[6] LEE J M, LEE C J, LEE K H, KIM B M. Effects of elastic−plastic properties of materials on residual indentation impressions in nano-indentation using sharp indenter [J]. Transactions of Nonferrous Metals Society of China, 2012, 22(3): 585−595.

[7] XIE G L, WANG Q S, MI X J, XIONG B Q, PENG L J. The precipitation behavior and strengthening of a Cu−2.0wt.%Be alloy [J]. Materials Science and Engineering A, 2012, 558: 326−330.

[8] MONTECINOS S, TOGNANA S, SALGUEIRO W. Influence of microstructure on the Young's modulus in a Cu−2Be (wt.%) alloy [J]. Journal of Alloys and Compounds, 2017, 729: 43−48.

[9] TANG Y, KANG Y, YUE L, JIAO X. Mechanical properties optimization of a Cu−Be−Co−Ni alloy by precipitation design [J]. Journal of Alloys and Compounds, 2017, 695: 613−625.

[10] YAGMUR L. Effect of microstructure on internal friction and Young's modulus of aged Cu−Be alloy [J]. Materials Science and Engineering A, 2009, 523(1−2): 65−69.

[11] RIOJA R J, LAUGHLIN D E. The sequence of precipitation in Cu−2wt%/Be alloys [J]. Acta Metallurgica, 1980, 28: 1301−1313.

[12] CHAKRABARTI D J, LAUGHLIN D E, TANNER L E. The Be−Cu (beryllium−copper) system [J]. Bulletin of Alloy Phase Diagrams, 1987, 8(3): 269−288.

[13] KHACHATURYAN A G, LAUGHLIN D E. Structural transformations during decomposition in CuBe alloys [J]. Acta Metallurgica et Materialia, 1990, 38(10): 1823−1835.

[14] VARSCHAVSKY A, DONOSO E. A differential scanning calorimetric study of precipitation in Cu_2Be [J]. Termochimica Acta, 1995, 266: 257−275.

[15] ZHOU Y J, SONG K X, XING J D, ZHANG Y M. Precipitation behavior and properties of aged Cu−0.23Be−0.84Co alloy [J]. Journal of Alloys and Compounds, 2016, 658: 920−930.

[16] MONTECINOS S, TOGNANA S, SALGUEIRO W. Determination of the Young's modulus in CuAlBe shape memory alloys with different microstructures by impulse excitation technique [J]. Materials Science and Engineering A, 2016, 676: 121−127.

[17] YAGMUR L, DUYGULU O, AYDEMIR B. Investigation of metastable γ' precipitate using HRTEM in aged Cu−Be alloy [J]. Materials Science and Engineering A, 2011, 528(12): 4147−4151.

[18] FISCHER-CRIPPS A C. A review of analysis methods for sub-micron indentation testing [J]. Vacuum, 2000, 58: 569−585.

[19] KIM B M, LEE C J, LEE J M. Estimations of work hardening exponents of engineering metals using residual indentation profiles of nano-indentation [J]. Journal of Mechanical Science and Technology, 2010, 24: 73−76.

[20] CHENG Y T, CHENG C M. Effects of 'sinking in' and 'piling up' on estimating the contact area under load in indentation [J]. Philosophical Magazine Letters, 1998, 78(2): 115−120.

[21] CHENG Y T, CHENG C M. What is indentation hardness? [J]. Surface and Coatings Technology, 2000, 133−134: 417−424.

[22] PANG J C, DUAN Q Q, WU S D, LI S X, ZHANG Z F. Fatigue strengths of Cu−Be alloy with high tensile strengths [J]. Scripta Materialia, 2010, 63: 1085−1088.

[23] QIAN L, LI M, ZHOU Z, YANG H, SHI X. Comparison of nano-indentation hardness to microhardness [J]. Surface and Coatings Technology, 2005, 195: 264−271.

[24] ZHANG P, LI S X, ZHANG Z F. General relationship between strength and hardness [J]. Materials Science and Engineering A, 2011, 529: 62−73.

[25] DAO M, CHOLLACOOP N, van VLIET K J, VENKATESH T A, SURESH S. Computational modeling of the forward and reverse problems in instrumented sharp indentation [J]. Acta Materialia, 2001, 49: 3899−3918.

[26] LOUBET J L, BAUER M, TONCK A, BEC S, GAUTHIER-MANUEL B. Nano-indentation with a surface force apparatus [M]. Dordrecht: Springer, 1993: 429−447.

[27] GUILLONNEAU G, KERMOUCHE G, BERGHEAU J M, LOUBET J L. A new method to determine the true projected contact area using nanoindentation testing [J]. Comptes Rendus Mecanique, 2015, 343: 410−418.

[28] NIX W D, GAO H. Indentation size effects in crystalline materials: A law for strain gradient plasticity [J]. Journal of the Mechanics and Physics of Solids, 1998, 46(3): 411−425.

[29] N'JOCK M Y, ROUDET F, IDRISS M, BARTIER O, CHICOT D. Work-of-indentation coupled to contact stiffness for calculating elastic modulus by instrumented indentation [J]. Mechanics of Materials, 2016, 94: 170−179.

[30] CHEN J, BULL S J. Relation between the ratio of elastic work to the total work of indentation and the ratio of hardness to Young's modulus for a perfect conical tip [J]. Journal of Materials Research, 2009, 24(3): 590−598.

[31] GIANNAKOPOULOS A E, SURESH S. Determination of elasto-plastic properties by instrumented sharp indentation [J]. Scripta Materialia, 1999, 40(10): 1191−1198.

凸起对纳米压痕测量含析出相的 Cu−2wt.%Be 的影响

S. MONTECINOS[1,2], S. TOGNANA[1,3,4], W. SALGUEIRO[1,3,4]

1. IFIMAT, Facultad de Ciencias Exactas, Universidad Nacional del Centro de la Provincia de Buenos Aires, Pinto 399, 7000 Tandil, Argentina;
2. Consejo Nacional de Investigaciones Científicas y Técnicas CONICET, Av. Rivadavia 1917, C1033AAJ Buenos Aires, Argentina;
3. CIFICEN (UNCPBA-CICPBA-CONICET), Pinto 399, 7000 Tandil, Argentina;
4. Comisión de Investigaciones Científicas de la Provincia de Bs. As., Calle 526 entre 10 y 11, 1900 La Plata, Argentina

摘　要：研究凸起对具有纳米析出相的 Cu−2wt.%Be 纳米压痕测量分析的影响。将样品在 540~680 K 之间的不同温度下时效 1 h，析出相形成。用经典的 Oliver 和 Pharr 法对载荷−深度曲线进行分析，并将得到的弹性模量和硬度值与其他技术估算的值进行比较。在具有析出相的样品中发现了重要的凸起水平，且观察到时效和未时效处理样品的载荷−深度曲线也不同。用 Loubet 模型估算硬度值，该模型在考虑有凸起的情况下，对接触深度进行修正。利用卸载功与压痕总功之比与 H/E_r(H 为硬度，E 为折合模量)比之间的关系确定弹性模量，并建立这两个参数间的特殊关系。

关键词：凸起；纳米压痕测量；铜合金；析出；显微组织；力学性能

(Edited by Wei-ping CHEN)